International Journal of General Medicine

Dovepress
Taylor & Francis Group

Open Access Full Text Article

ORIGINAL RESEARCH

Multi-Modality Ultrasound Model for Renal Fibrosis Assessment in Chronic Kidney Disease: Integrating Grayscale and Color Doppler Ultrasound Radiomics with Shear Wave Elastography

Ziman Chen[1,*], Chaoqun Wu[2,3,*], Yingli Wang[4]

[1]Department of Health Technology and Informatics, the Hong Kong Polytechnic University, Kowloon, Hong Kong; [2]Department of Ultrasound, the First Affiliated Hospital of Wenzhou Medical University, Wenzhou, People's Republic of China; [3]Department of Ultrasound, the Fifth Affiliated Hospital of Sun Yat-Sen University, Zhuhai, People's Republic of China; [4]Ultrasound Department, EDAN Instruments, Inc., Shenzhen, People's Republic of China

*These authors contributed equally to this work

Correspondence: Ziman Chen, Department of Health Technology and Informatics, the Hong Kong Polytechnic University, Kowloon, Hong Kong, Email chenzm27@alumni.sysu.edu.cn

Objective: Accurate assessment of renal fibrosis is critical for managing chronic kidney disease (CKD). This study aimed to develop a multi-modality ultrasound-based model that integrates radiomics signatures derived from grayscale ultrasound and color Doppler ultrasound, along with shear wave elastography (SWE) measurements, to assess the severity of renal fibrosis in CKD patients.

Methods: A total of 125 CKD patients were enrolled and classified into mild and moderate-to-severe fibrosis groups based on renal biopsy. Radiomics features were extracted from grayscale and color Doppler ultrasound images, and key features were identified using machine learning algorithms to construct radiomics signatures for each modality. SWE measurements were used to assess renal stiffness. A multi-modality ultrasound model was constructed using logistic regression, combining the dual-modality radiomics signatures with SWE data. Model performance was evaluated using receiver operating characteristic (ROC) curves, five-fold cross-validation, calibration, and decision curve analysis (DCA).

Results: Individual modalities for SWE, grayscale ultrasound radiomics, and color Doppler ultrasound radiomics showed area under the ROC curves (AUCs) of 0.74 (95% CI: 0.65–0.82), 0.79 (95% CI: 0.71–0.87), and 0.70 (95% CI: 0.60–0.79), respectively. The multi-modality model, integrating all three modalities, achieved an AUC of 0.88 (95% CI: 0.82–0.94), sensitivity of 0.82 (95% CI: 0.70–0.91), specificity of 0.84 (95% CI: 0.73–0.92), and accuracy of 0.83 (95% CI: 0.75–0.89). In cross-validation, the model showed robust generalizability (AUC: 0.89, 95% CI: 0.74–1.00). The calibration curve showed excellent agreement between predicted and observed outcomes, and the DCA curve confirmed the clinical utility of the model. A nomogram based on the multi-modality model was developed for individualized risk assessment of moderate-to-severe renal fibrosis.

Conclusion: The multi-modality ultrasound model enhances non-invasive renal fibrosis assessment in CKD patients. By combining dual-modality radiomics with SWE measurements, this model offers a promising tool for personalized clinical decision-making and better management of CKD progression.

Keywords: chronic kidney disease, renal fibrosis, ultrasound, shear wave elastography

Introduction

Chronic kidney disease (CKD) is an escalating global health issue, affecting over 800 million individuals worldwide—more than 10% of the global population.[1,2] The morbidity of CKD is steadily increasing, with projections indicating it

Received: 30 July 2025
Accepted: 11 October 2025
Published: 18 October 2025

will become the fifth leading cause of death globally by 2040.[3] Renal fibrosis, a key pathological hallmark of CKD, is characterized by the progressive deposition of extracellular matrix components, leading to renal scarring and functional decline.[4,5] As a critical driver of disease progression, renal fibrosis significantly contributes to poor clinical outcomes, including the deterioration of kidney function and eventual progression to end-stage renal disease.[6] Given its pivotal role in advancing CKD, accurate and timely assessment of renal fibrosis is essential for monitoring disease progression and guiding clinical decision-making.

Ultrasound is widely used as the first-line imaging modality for kidney evaluation due to its non-invasive nature, cost-effectiveness, and lack of ionizing radiation.[7] While conventional ultrasound can detect gross structural changes and assess renal hemodynamics, it is limited in evaluating the extent of fibrosis, especially in the early stages of the disease, when fibrosis may not yet cause significant structural damage or changes in renal blood flow and perfusion. Shear wave elastography (SWE) has emerged as a promising non-invasive modality for assessing tissue stiffness, including in renal tissues.[8] This technique applies an acoustic radiation force impulse (ARFI) to the tissue, generating shear waves that propagate through the medium. The velocity at which these waves travel is directly proportional to tissue stiffness, and the resulting data can be used to generate a color-coded elastogram reflecting the mechanical properties of the tissue. SWE has demonstrated considerable potential in evaluating fibrosis in various organs, such as the liver, and has recently been investigated for renal fibrosis.[9,10] By quantifying kidney stiffness, SWE provides valuable insights into fibrosis, which may not be detectable with conventional imaging techniques.

In recent years, radiomics has emerged as an innovative approach in medical imaging, enabling the extraction of large volumes of quantitative features from medical images that are not visible to the naked eye.[11,12] This technique uses advanced machine learning algorithms to analyze medical images and extract a wide range of radiomics features, such as texture, shape, and statistical properties, which can characterize tissue heterogeneity. Radiomics has shown significant promise in diagnosing, prognosticating, and planning treatment for various diseases.[13–15] However, its application in assessing renal fibrosis in CKD patients remains relatively underexplored. Our research team has previously developed a radiomics-based model using grayscale ultrasound images to evaluate the severity of renal fibrosis in CKD patients.[16] This model demonstrated promising potential for non-invasive fibrosis assessment, although it was limited to grayscale imaging, which offers relatively limited diagnostic information.

Recent studies have highlighted the potential of integrating multiple ultrasound modalities to enhance diagnostic accuracy.[17,18] Color Doppler ultrasound, which provides valuable insights into blood flow and tissue perfusion, can offer complementary information to enrich other imaging features. However, most existing approaches extract radiomic features from composite color Doppler images without considering the distinct contributions of the red, green, and blue (RGB) channels.[19,20] This may overlook subtle variations in blood flow patterns that could be critical for fibrosis assessment. Additionally, while SWE has been increasingly used to quantify tissue stiffness, prior attempts to apply radiomics to SWE images have faced challenges due to the inherent variability in elastogram acquisition and interpretation, particularly in regions such as the renal poles and medulla.[21,22] In contrast, direct SWE-derived quantitative elasticity measurements from the renal cortex—where stiffness assessment is most reliable—may provide more consistent and clinically meaningful data.[23]

Thus, in this study, we aim to develop an integrated model that combines radiomics signatures derived from both grayscale and color Doppler ultrasound images—with features extracted separately from the RGB channels to optimize hemodynamic characterization—along with direct SWE elasticity measurements for renal fibrosis assessment in CKD patients. By leveraging these methodological refinements, we seek to construct a robust diagnostic tool that enhances the accuracy of fibrosis assessment and enables more effective monitoring of disease progression.

Materials and Methods

Ethical Statement

This study was approved by the Ethics Committee of our institution and conducted in accordance with the Declaration of Helsinki. All participants provided written informed consent prior to inclusion.

Study Population

This single-center, prospective, cross-sectional study was conducted between April 2019 and June 2022. Patients with CKD who underwent renal ultrasound examination and kidney biopsy at our institution were consecutively enrolled. Inclusion criteria were: (1) diagnosis of CKD according to the Kidney Disease Improving Global Outcomes (KDIGO) 2012 guidelines; (2) availability of pre-biopsy renal ultrasound images, including grayscale ultrasound, color Doppler ultrasound, and SWE; and (3) availability of renal biopsy specimens for fibrosis evaluation. Exclusion criteria included: (1) presence of conditions such as polycystic kidney disease, hydronephrosis, renal masses, or calculi that could interfere with image acquisition; (2) poor quality ultrasound images precluding accurate analysis; and (3) insufficient biopsy specimens that could not be evaluated for renal fibrosis.

The study workflow is presented in Figure 1.

Ultrasound Examination and Renal Biopsy

Ultrasound examinations were performed using the Aixplorer Ultrasound Imaging System (SuperSonic Imagine, Aix-en-Provence, France), equipped with a linear array transducer (SL15-4, 4–15 MHz). All procedures were conducted independently by an experienced radiologist. Grayscale and color Doppler ultrasonography were first employed to assess renal structure and blood flow. Longitudinal kidney images were obtained in both grayscale and color Doppler modes for subsequent radiomics analysis. SWE was then used to assess the elasticity of the renal cortex in the mid-portion of the kidney, with the maximum elasticity value (Emax) recorded, as it is known to have optimal diagnostic performance for evaluating different degrees of renal fibrosis.[10]

Ultrasound-guided renal biopsy was performed on the lower pole of the kidney to obtain tissue samples for semi-quantitative renal fibrosis assessment.[10] For analysis, the moderate and severe renal fibrosis groups were combined into a single moderate-to-severe group and compared with the mild fibrosis group.

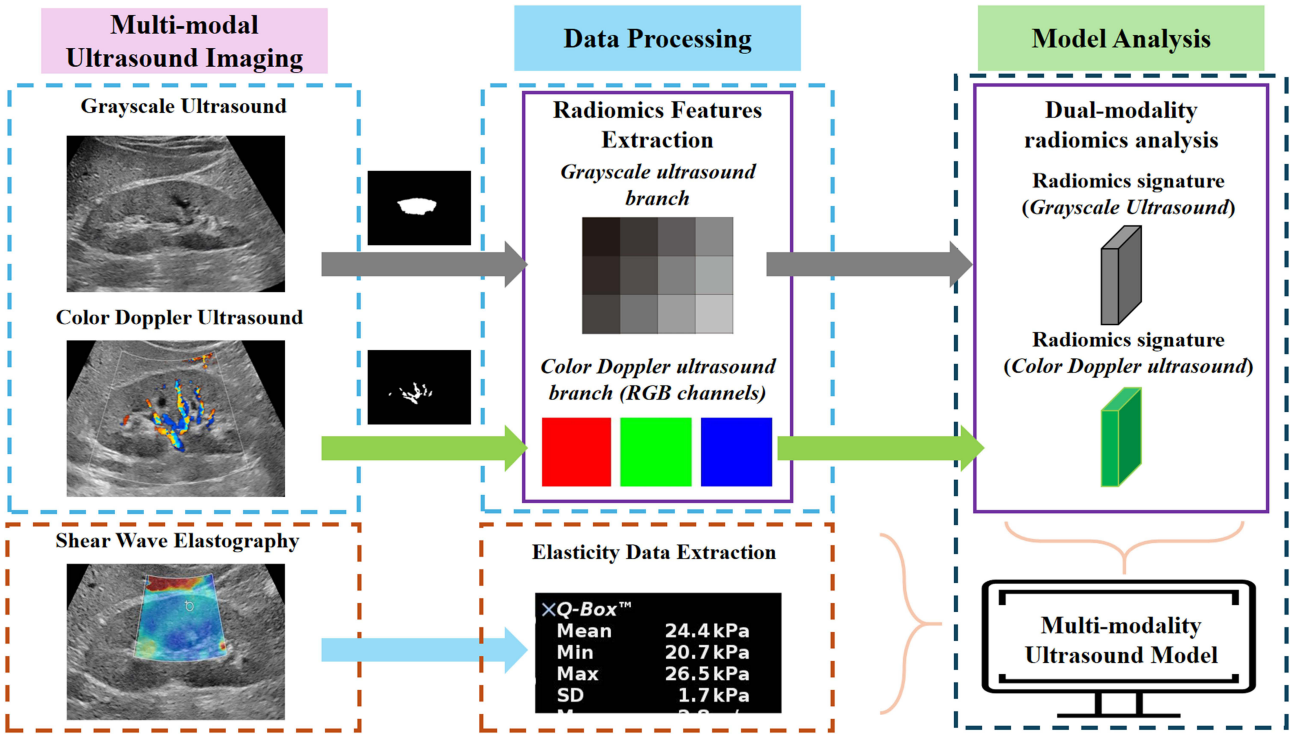

Figure 1 Workflow of the multi-modality ultrasound model. Radiomics features were extracted separately from grayscale and color Doppler ultrasound images (with RGB channels processed individually) to generate modality-specific radiomics signatures. These dual-modality radiomics signatures were then integrated with quantitative elasticity data from shear wave elastography to construct the final model.

https://doi.org/10.2147/IJGM.S557196

Radiomics Feature Extraction, Selection, and Model Construction

Radiomics features were extracted from grayscale and color Doppler ultrasound images using the open-source Python package Pyradiomics. The region of interest (ROI) was manually delineated by a radiologist with six years of experience in ultrasound radiomics, covering the renal cortex on grayscale images and the blood flow signal areas on color Doppler images. From grayscale images, radiomics features included first-order statistical measures as well as texture-based features. From color Doppler images, radiomics features were extracted separately from each of the RGB channels to capture variations in pixel intensity and texture across the color spectrum. Both the original and filtered images (via Laplacian of Gaussian filters and wavelet transformations) were processed to enhance feature diversity.

A four-step strategy was employed for feature dimensionality reduction and selection. First, low-variance features were discarded, as they provided minimal discriminative value. Next, highly correlated features (Spearman correlation coefficient > 0.9) were removed to reduce redundancy. The remaining features were refined using the Minimum Redundancy Maximum Relevance (mRMR) algorithm, selecting the top 50 features with high relevance to the outcome while minimizing redundancy. Finally, Least Absolute Shrinkage and Selection Operator (Lasso) regression was applied to further narrow the feature set, retaining the most relevant features for analysis.

Separate radiomics signatures were constructed for the grayscale ultrasound and color Doppler ultrasound images using the selected radiomics features. These signatures, along with the SWE value, were then used to construct a multi-modality ultrasound model, which was built using a logistic regression algorithm.

In addition, we evaluated the consistency of the extracted key radiomics features. The radiologist randomly selected ultrasound images from 30 cases and performed a repeatability analysis one week later to assess intra-observer consistency. Additionally, another radiologist with five years of experience in radiomics analysis conducted the same analysis on the selected cases to evaluate inter-observer consistency.

Model Evaluation

The diagnostic performance of the radiomics signatures, SWE imaging, and the multi-modality ultrasound model was evaluated using receiver operating characteristic (ROC) curves. Sensitivity, specificity, and accuracy were calculated to assess the diagnostic performance. To validate the constructed models, five-fold cross-validation was employed. In five-fold cross-validation, the dataset was randomly divided into five subsets. The model was trained on four subsets and tested on the remaining subset. This process was repeated five times to ensure each subset served as a test set once, promoting a more generalized evaluation of the model's performance.

Additionally, a calibration curve was constructed to assess the predictive accuracy of the model by comparing predicted probabilities with observed outcomes. Decision curve analysis (DCA) was employed to evaluate the clinical benefit of the model by considering net benefits at various threshold probabilities for decision-making.

A nomogram was developed based on the multi-modality ultrasound model to visually represent predictions. The nomogram incorporates radiomics signatures from grayscale ultrasound, color Doppler ultrasound, and the SWE value, facilitating individualized risk assessment. The total score derived from the model was used to estimate the probability of moderate-to-severe renal fibrosis, offering a user-friendly tool for clinical decision-making.

Statistical Analysis

Statistical analyses were performed using Python version 3.11.4 and R software version 4.4.0. Categorical variables were presented as counts (percentages), while continuous variables were expressed as means ± standard deviations (SD) or medians with interquartile ranges (IQRs) depending on data distribution. A two-sided P value of < 0.05 was considered statistically significant.

Results

Study Population

A total of 125 patients with CKD were enrolled in this study. Among them, 64 patients were classified as having mild fibrosis, while 61 patients were classified with moderate-to-severe fibrosis. The mean age of the mild fibrosis group was

Table 1 Baseline Characteristics of Study Cohort

Characteristic	Mild Fibrosis (n = 64)	Moderate-to-Severe Fibrosis (n = 61)
Age (years)	33.30 ± 12.79	44.89 ± 14.84
Gender	36 (56.25)	34 (55.74)
Male	28 (43.75)	27 (44.26)
Female		
SWE (kPa)	39.36 ± 9.77	30.61 ± 9.03
Radiomics_grayscale	−0.18 (−0.37–0.04)	0.11 (−0.08–0.23)
Radiomics_colordoppler	−0.19 (−0.35–0.03)	0.01 (−0.20–0.29)

Notes: Categorical variables are presented as n (%) and continuous variables as mean ±standard deviation or median (interquartile range). Radiomics_grayscale = radiomics features extracted from grayscale ultrasound images; Radiomics_colordoppler = radiomics features extracted from color Doppler ultrasound images.
Abbreviation: SWE, shear wave elastography.

33.30 ± 12.79 years, while the mean age of the moderate-to-severe fibrosis group was 44.89 ± 14.84 years. The baseline characteristics of the study population are summarized in Table 1.

Radiomics Feature Extraction and Selection

A total of 651 radiomics features were extracted from grayscale ultrasound images. Similarly, 651 radiomics features were extracted separately from the R, G, and B channels of color Doppler ultrasound images, resulting in a total of 1953 features. Using a four-step strategy, four significant radiomics features were identified from grayscale ultrasound images, while six significant radiomics features were selected from color Doppler ultrasound images (Table S1). These features were then linearly combined based on their coefficients to construct the grayscale ultrasound radiomics signature and color Doppler ultrasound radiomics signature, respectively. Additionally, consistency analysis demonstrated favorable reproducibility of the extracted key radiomics features, with an intraclass correlation coefficient greater than 0.80.

Diagnostic Performance of Shear Wave Elastography and Radiomics Signatures

SWE demonstrated moderate diagnostic performance, with an AUC of 0.74 (95% CI: 0.65–0.82). The sensitivity was 0.79 (95% CI: 0.66–0.88), specificity was 0.61 (95% CI: 0.48–0.73), and accuracy was 0.70 (95% CI: 0.61–0.78). Grayscale ultrasound radiomics signature showed a higher AUC of 0.79 (95% CI: 0.71–0.87), with sensitivity of 0.57 (95% CI: 0.44–0.70), specificity of 0.88 (95% CI: 0.77–0.94), and accuracy of 0.73 (95% CI: 0.64–0.80). In contrast, color Doppler ultrasound radiomics signature had an AUC of 0.70 (95% CI: 0.60–0.79), with sensitivity of 0.66 (95% CI: 0.52–0.77), specificity of 0.69 (95% CI: 0.56–0.80), and accuracy of 0.67 (95% CI: 0.58–0.75) (Table 2).

Diagnostic Performance of the Constructed Multi-Modality Model

The multi-modality model, integrating radiomics signatures from both grayscale and color Doppler ultrasound along with SWE measurements, outperformed individual modalities in terms of diagnostic performance (Table 3). This model achieved an AUC of 0.88 (95% CI: 0.82–0.94), sensitivity of 0.82 (95% CI: 0.70–0.91), specificity of 0.84 (95% CI:

Table 2 Diagnostic Performance of Shear Wave Elastography and Radiomics Signatures

Index	Sensitivity (95% CI)	Specificity (95% CI)	Accuracy (95% CI)	AUC (95% CI)
SWE	0.79 (0.66–0.88)	0.61 (0.48–0.73)	0.70 (0.61–0.78)	0.74 (0.65–0.82)
Radiomics_grayscale	0.57 (0.44–0.70)	0.88 (0.77–0.94)	0.73 (0.64–0.80)	0.79 (0.71–0.87)
Radiomics_colordoppler	0.66 (0.52–0.77)	0.69 (0.56–0.80)	0.67(0.58–0.75)	0.70 (0.60–0.79)

Notes: Radiomics_grayscale = radiomics features extracted from grayscale ultrasound images; Radiomics_colordoppler = radiomics features extracted from color Doppler ultrasound images.
Abbreviations: SWE, shear wave elastography; AUC, area under the curve; CI, confidence interval.

Table 3 Diagnostic Performance of the Constructed Multi-Modality Model

Index	Sensitivity (95% CI)	Specificity (95% CI)	Accuracy (95% CI)	AUC (95% CI)
Multi-modality model	0.82 (0.70–0.91)	0.84 (0.73–0.92)	0.83 (0.75–0.89)	0.88 (0.82–0.94)
5-folds cross-validation	0.77 (0.63–0.91)	0.80 (0.71–0.89)	0.78 (0.74–0.82)	0.89 (0.74–1.00)

Abbreviations: AUC, area under the curve; CI, confidence interval.

0.73–0.92), and accuracy of 0.83 (95% CI: 0.75–0.89) (Figures 2 and 3). In the five-fold cross-validation, the model demonstrated robust performance, with sensitivity of 0.77 (95% CI: 0.63–0.91), specificity of 0.80 (95% CI: 0.71–0.89), and an AUC of 0.89 (95% CI: 0.74–1.00), further confirming its generalizability (Figure 4).

In addition, we constructed a baseline model including age and SWE for comparison. This baseline model achieved an AUC of 0.83 (95% CI: 0.76–0.90). Compared with this baseline, the multi-modality model demonstrated higher discrimination. Importantly, reclassification analyses showed that the multi-modality model significantly improved patient-level risk assessment, with a continuous net reclassification improvement (NRI) of 65.5% (95% CI: 32.4%–98.7%, $P < 0.001$) and an integrated discrimination improvement (IDI) of 12.4% (95% CI: 3.0%–21.8%, $P = 0.010$), indicating that the inclusion of radiomics signatures provided meaningful incremental value.

To further illustrate the contribution of individual variables, a feature importance analysis was performed. As shown in Figure 5, the grayscale radiomics signature contributed most substantially to the final model, followed by SWE and the color Doppler radiomics signature.

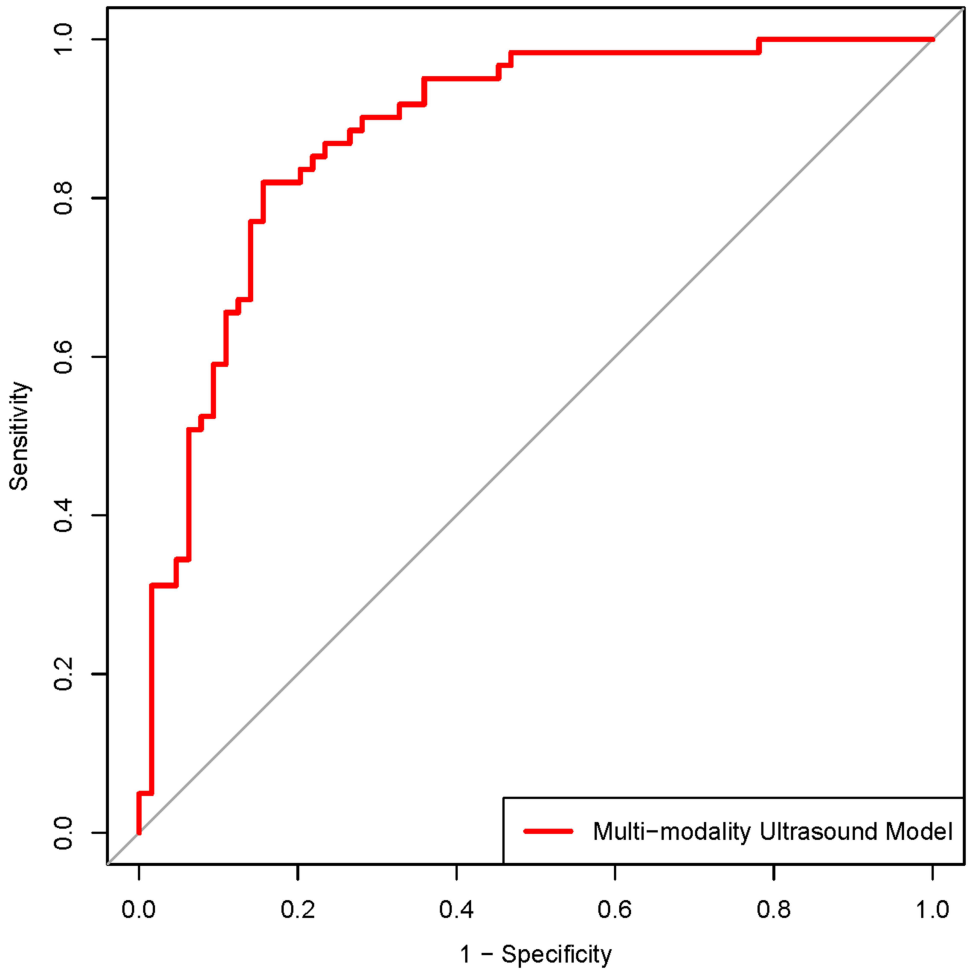

Figure 2 ROC curve for the constructed multi-modality ultrasound model.

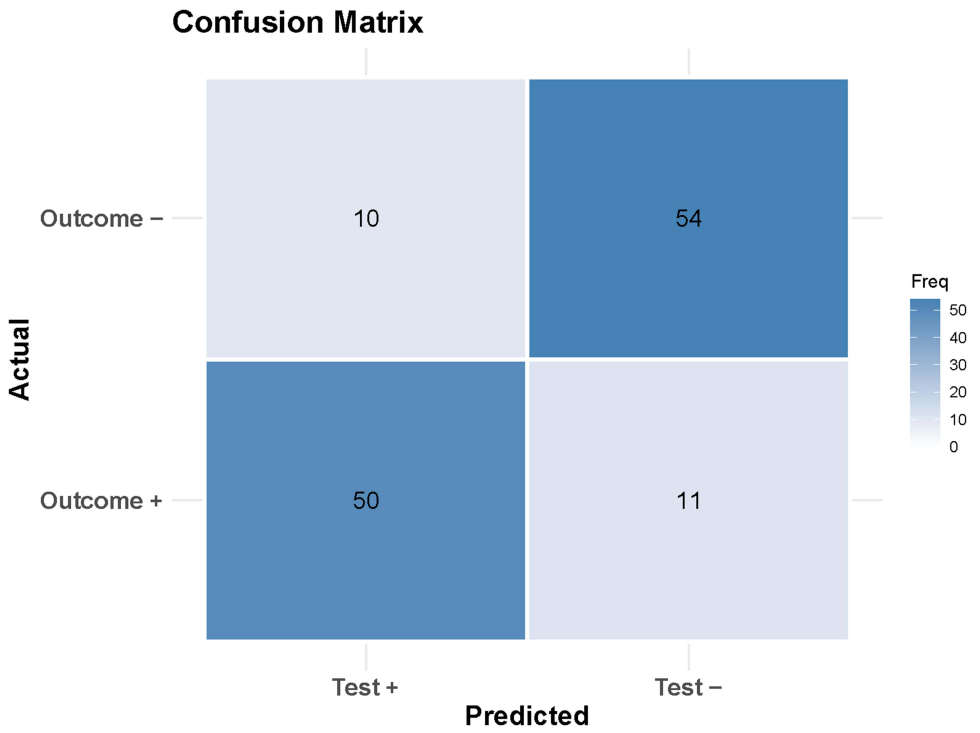

Figure 3 Confusion matrix for the constructed multi-modality ultrasound model.

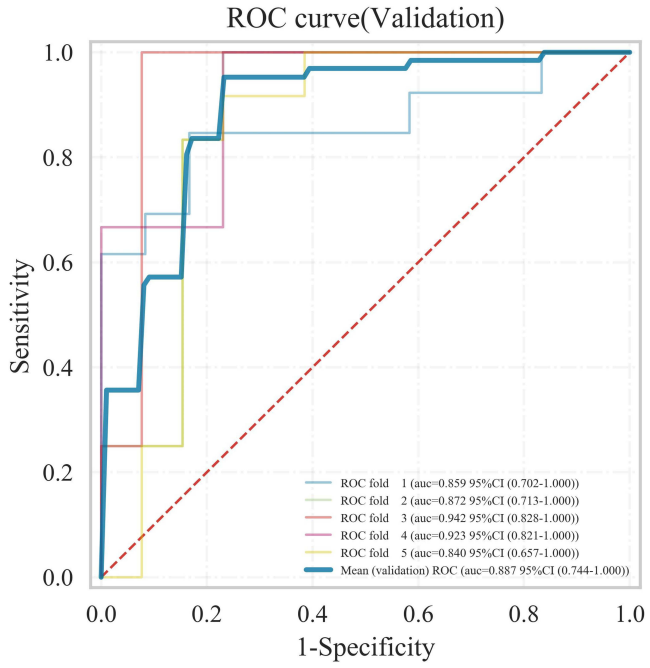

Figure 4 ROC curves of the five-fold cross-validation for the constructed multi-modality ultrasound model.

The diagnostic performance of the multi-modality model was validated using a calibration curve (Figure 6), which demonstrated good agreement between predicted probabilities and observed outcomes (Hosmer-Lemeshow test: P = 0.625). DCA curve (Figure 7) illustrated that the multi-modality model provided a significant net benefit across a range of threshold probabilities, supporting its clinical utility. A nomogram based on the multi-modality model was developed

https://doi.org/10.2147/IJGM.S557196

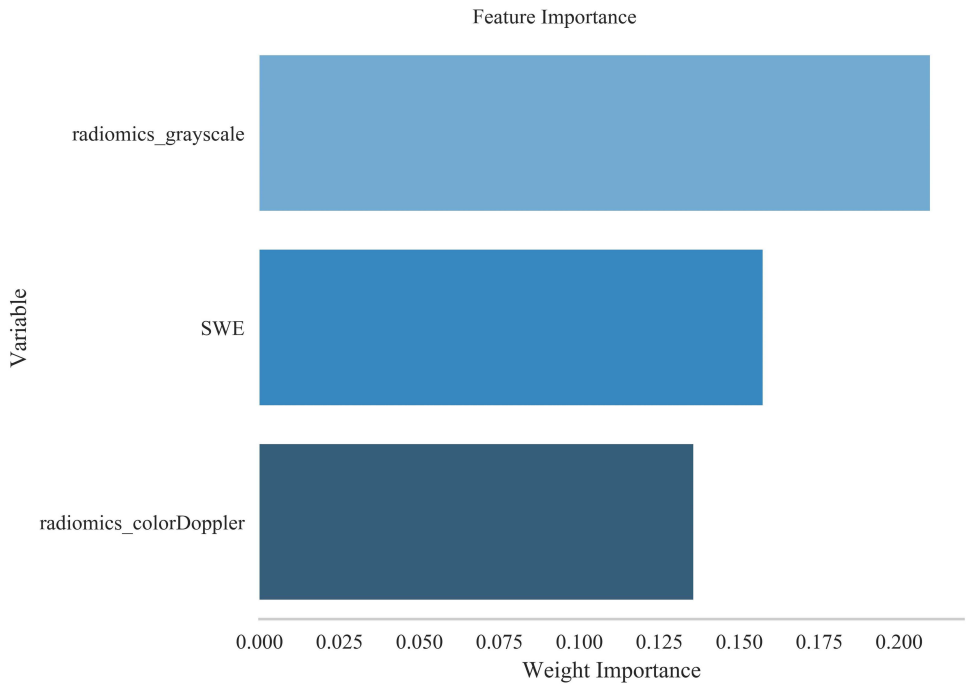

Figure 5 Relative importance of variables in the multi-modality ultrasound model. The grayscale radiomics signature contributed most substantially to the model, followed by SWE and the color Doppler radiomics signature.

as a practical tool for individualized risk assessment, enabling clinicians to estimate the likelihood of moderate-to-severe renal fibrosis in CKD patients (Figure 8). This nomogram integrates radiomics signatures from grayscale ultrasound, color Doppler ultrasound, and SWE values, offering a user-friendly, evidence-based approach to support clinical decision-making and personalized treatment strategies.

Discussion

In this study, we proposed a multi-modality ultrasound model for assessing renal fibrosis in CKD patients. By integrating radiomics signatures from both grayscale and channel-separated color Doppler ultrasound images with SWE measurements, our model demonstrated significant clinical value and outperformed individual imaging modalities in diagnostic performance. These findings suggest that combining dual-modality ultrasound radiomics with SWE data enables a more comprehensive and reliable approach to renal fibrosis assessment, which is crucial for timely and accurate diagnosis in CKD patients.

Radiomics, when integrated with machine learning techniques, involves extracting high-throughput features from medical images to quantify the inherent heterogeneity of diseases, enabling a more detailed exploration of their manifestations.[24] While radiomics has shown promise in ultrasound-based renal disease analysis, previous approaches have faced limitations in fully capturing disease-specific signatures. For instance, Qin et al developed a dual-modality model based on grayscale ultrasound and color Doppler ultrasound radiomics analysis to classify the severity of renal fibrosis in CKD patients.[25] Although their work established the value of multi-parametric analysis, the color Doppler component treated the composite image as a single dataset, potentially diluting critical hemodynamic information encoded in individual color channels. Zhu et al emphasized that separate processing of the R, G, and B channels in color Doppler images preserved directional flow signatures critical for microvascular assessment[26]—a finding that directly informed our methodological approach. Notably, color Doppler images are a form of pseudo-color representation that encode hemodynamic information, with flow direction represented by color (blue for flow away from the transducer and red for flow toward it), mean velocity indicated by brightness, and turbulence or variance reflected in a third color (often green).[27] Conventional radiomics approaches that extract features directly from composite images may conflate these distinct hemodynamic properties. By analyzing R, G, and B channels separately, our method retains the biophysical

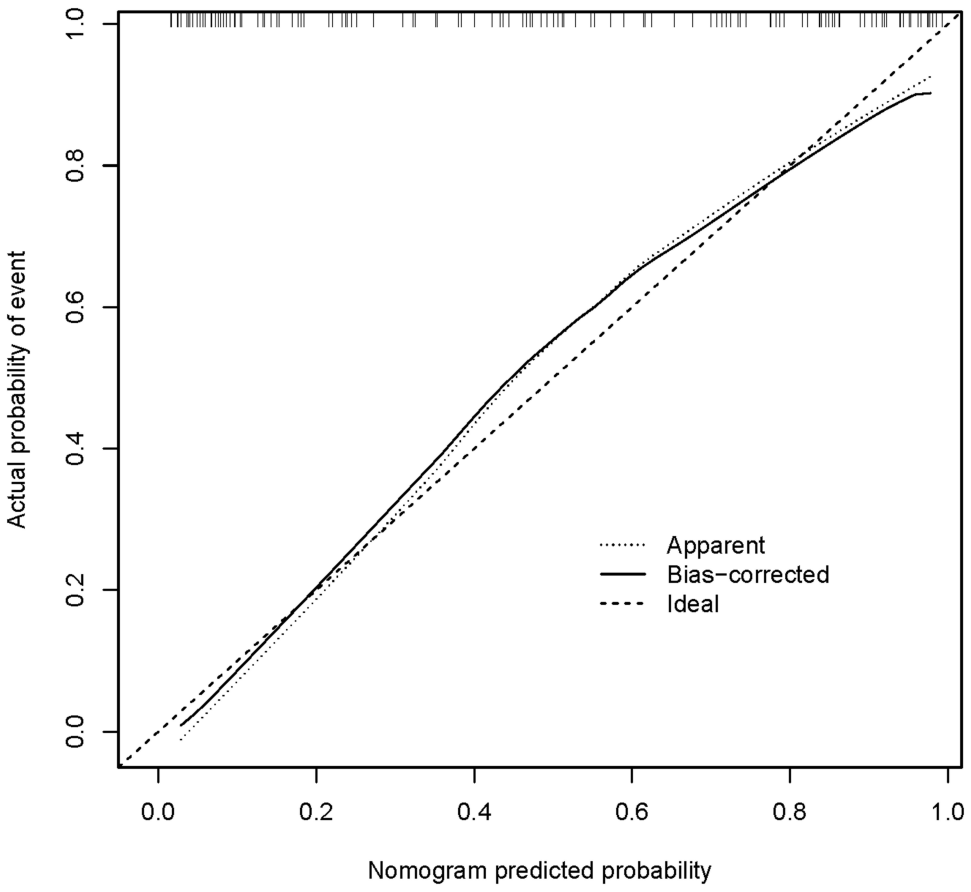

Figure 6 Calibration plot for the constructed multi-modality ultrasound model.

meaning of different flow patterns—particularly crucial for detecting fibrotic microvascular remodeling characterized by subtle perfusion changes. This channel-specific approach minimized information loss from color mapping and allowed our model to identify subtle flow alterations that would be averaged out in traditional analyses.

In the present study, we opted not to extract radiomics features from elastography images due to fundamental technical constraints inherent to renal SWE imaging. The accuracy of elastography is influenced by several factors, particularly the interaction between ARFI, orientation of the target tissue, and the shear wave propagation direction.[28] Variability can arise when the angle between ARFI and the shear wave propagation deviates from the optimal direction, leading to measurement inaccuracies. This issue is particularly pronounced in regions such as the renal poles and medulla, where tissue orientation and the angle of the ultrasound beam can induce significant anisotropy.[29–31] While elastograms provide valuable visual representations of tissue stiffness, their use for radiomics analysis inherently incorporates these problematic anisotropic regions. This methodological limitation is especially consequential in renal applications, where prior studies have established that reliable stiffness assessment requires strict adherence to standardized measurement protocols.[23,32] Given these technical constraints, direct elastography measurements demonstrate superior clinical utility for renal fibrosis assessment by enabling targeted stiffness quantification in optimal measurement regions while excluding anisotropic areas. This approach yields more robust and reproducible biomechanical biomarkers compared to radiomics features derived from elastography images, as the latter require analysis across larger image areas where anisotropic regions cannot be reliably excluded, thereby introducing significant confounding variables.

The synergy between these modalities is particularly noteworthy. The grayscale radiomics signature primarily reflects textural heterogeneity associated with extracellular matrix deposition, while the Doppler channel-separated features provide complementary information about microvascular architecture. SWE measurements then add a biomechanical dimension by quantifying tissue stiffness—a direct correlate of fibrotic burden. This multi-parametric approach mirrors

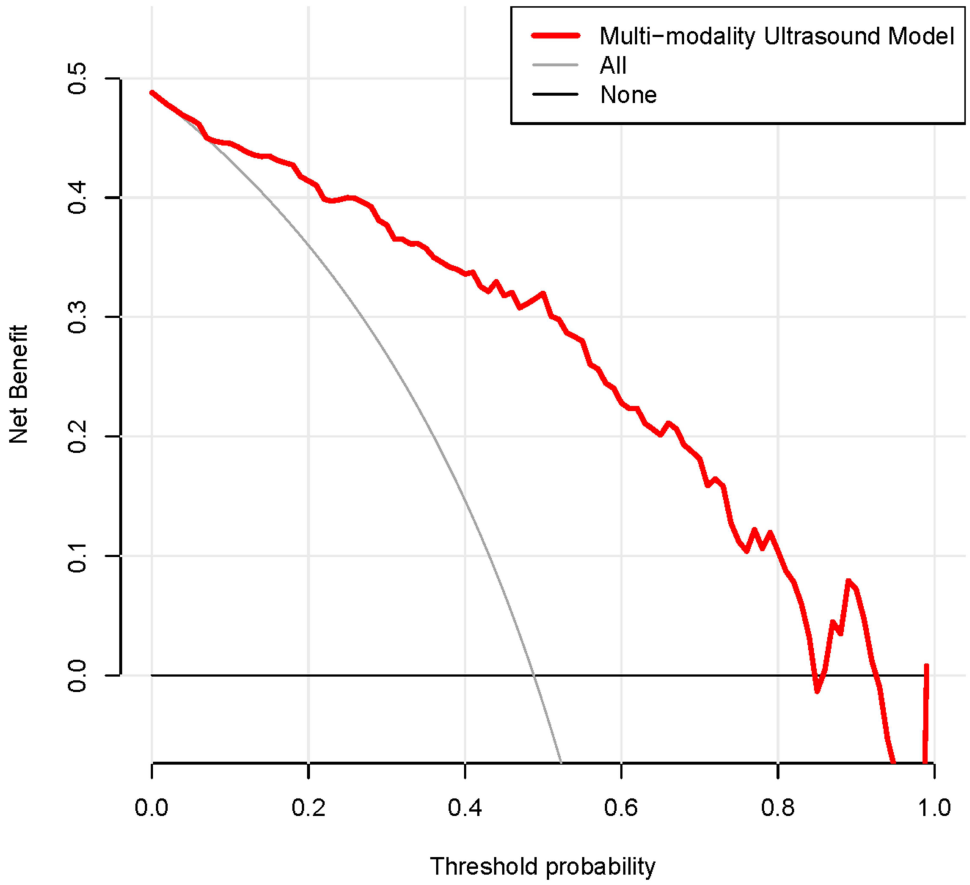

Figure 7 Decision curve analysis for the constructed multi-modality ultrasound model.

the complex pathophysiology of renal fibrosis, where structural, vascular, and mechanical changes occur concurrently but may not be equally detectable by any single modality. Such biological plausibility strengthens the clinical translatability of our model. Beyond ultrasound-based approaches, other imaging modalities have also been investigated for renal fibrosis assessment. Magnetic resonance elastography (MRE), for example, has demonstrated high diagnostic accuracy for assessing tissue stiffness and has been applied in both hepatic and renal fibrosis research.[33] However, the requirement for specialized equipment, longer acquisition times, higher costs, and limited availability constrain its widespread use in routine CKD management. In contrast, our multi-modality ultrasound model combines grayscale and color Doppler radiomics with SWE to provide a more accessible, cost-effective, and bedside-applicable tool. In addition, the nomogram derived from the multi-modality model provides a practical tool for individualized risk estimation in clinical practice. For instance, if the nomogram indicates an 85% probability of moderate-to-severe fibrosis, clinicians may be more inclined to recommend renal biopsy or initiate closer follow-up, whereas a low estimated probability (eg, 10%) could support a more conservative monitoring strategy. In this way, the nomogram may aid patient risk stratification and guide decision-making, thereby bridging the gap between quantitative imaging biomarkers and personalized CKD management.

While this study achieved promising results, there are several limitations. First, this was a single-center study, which may limit the generalizability of our findings across different patient populations and ultrasound platforms, as variations in demographics, disease spectrum, and equipment may influence model performance. Second, the sample size is relatively small for machine learning–based analysis. Nevertheless, our model included only three variables, and the events-per-variable (EPV) was approximately 20, which is well above the commonly recommended threshold of 10.[34] This suggests that the sample size was statistically adequate to support the model construction. Future research should validate the robustness and applicability of the model using multi-center, large-scale datasets that encompass diverse populations and ultrasound systems to enhance its external validity. Third, the extraction of radiomics features in this

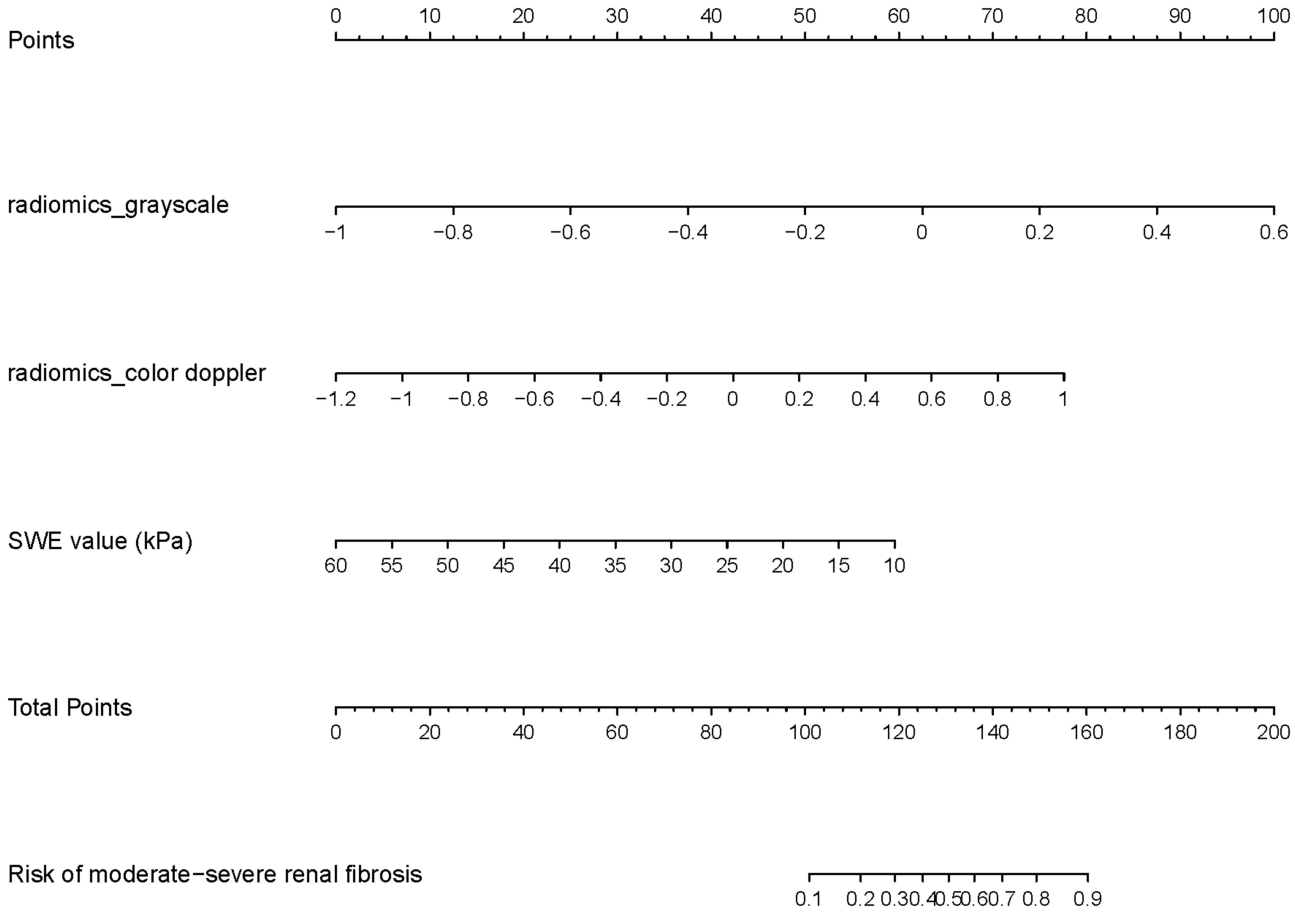

Figure 8 Nomogram for the constructed multi-modality ultrasound model.

study involved manual processing, which is prone to human bias and inconsistencies. The integration of automated or semi-automated feature extraction methods could minimize these biases and improve the reproducibility and scalability of the model. Finally, although the multimodal approach demonstrated high performance in the study, its real-world clinical application remains to be fully tested. The model's performance should be further evaluated across various ultrasound platforms, by different operators, and under diverse clinical conditions to ensure its widespread applicability and reliability in different healthcare settings. In addition, future research should explore whether these radiomics and elastography-derived features have prognostic value, such as predicting the rate of renal function decline over time, thereby extending the model's clinical utility from diagnosis to long-term patient management.

Conclusions

In conclusion, this study demonstrates that a multi-modality ultrasound model, integrating radiomics signatures from both grayscale and channel-separated color Doppler ultrasound with SWE measurements, can provide a more accurate, non-invasive method for assessing renal fibrosis in CKD patients. The model shows promise for improving CKD management by facilitating timely and more accurate diagnosis, better monitoring of disease progression, and may potentially aid in patient risk stratification to guide clinical decisions, such as the timing of biopsy. Future work should focus on external validation, model refinement, and exploring its clinical applicability in larger and more diverse healthcare settings.

Data Sharing Statement

The data presented in this study are available on reasonable request from the corresponding author. The data are not publicly available due to ethical concerns regarding privacy.

Ethical Approval

The study was conducted according to the Declaration of Helsinki guidelines, and approved by the Institutional Review Board (or Ethics Committee) of the Fifth Affiliated Hospital of Sun Yat-sen University (protocol code K09-1).

Acknowledgments

Thanks to Zhongzhen Su for valuable guidance in the study design.

Author Contributions

All authors made a significant contribution to the work reported, whether that is in the conception, study design, execution, acquisition of data, analysis and interpretation, or in all these areas; took part in drafting, revising or critically reviewing the article; gave final approval of the version to be published; have agreed on the journal to which the article has been submitted; and agree to be accountable for all aspects of the work.

Funding

This study was supported by the Hong Kong Polytechnic University (Ref no. P0056738).

Disclosure

The authors declare no conflicts of interest in this work.

References

1. Jager KJ, Kovesdy C, Langham R, Rosenberg M, Jha V, Zoccali C. A single number for advocacy and communication-worldwide more than 850 million individuals have kidney diseases. *Kidney Int*. 2019;96(5):1048–1050. doi:10.1016/j.kint.2019.07.012
2. Kovesdy CP. Epidemiology of chronic kidney disease: an update 2022. *Kidney Int Suppl*. 2022;12(1):7–11. doi:10.1016/j.kisu.2021.11.003
3. Foreman KJ, Marquez N, Dolgert A, et al. Forecasting life expectancy, years of life lost, and all-cause and cause-specific mortality for 250 causes of death: reference and alternative scenarios for 2016-40 for 195 countries and territories. *Lancet*. 2018;392(10159):2052–2090. doi:10.1016/s0140-6736(18)31694-5
4. Yuan Q, Tang B, Zhang C. Signaling pathways of chronic kidney diseases, implications for therapeutics. *Signal Transduct Target Ther*. 2022;7(1):182. doi:10.1038/s41392-022-01036-5
5. Rockey DC, Bell PD, Hill JA. Fibrosis–a common pathway to organ injury and failure. *N Engl J Med*. 2015;372(12):1138–1149. doi:10.1056/NEJMra1300575
6. Reiss AB, Jacob B, Zubair A, Srivastava A, Johnson M, De Leon J. Fibrosis in chronic kidney disease: pathophysiology and therapeutic targets. *J Clin Med*. 2024;13(7). doi:10.3390/jcm13071881
7. Singla RK, Kadatz M, Rohling R, Nguan C. Kidney ultrasound for nephrologists: a review. *Kidney Med*. 2022;4(6):100464. doi:10.1016/j.xkme.2022.100464
8. Shiina T, Nightingale KR, Palmeri ML, et al. WFUMB guidelines and recommendations for clinical use of ultrasound elastography: part 1: basic principles and terminology. *Ultrasound Med Biol*. 2015;41(5):1126–1147. doi:10.1016/j.ultrasmedbio.2015.03.009
9. Ferraioli G, Filice C, Castera L, et al. WFUMB guidelines and recommendations for clinical use of ultrasound elastography: part 3: liver. *Ultrasound Med Biol*. 2015;41(5):1161–1179. doi:10.1016/j.ultrasmedbio.2015.03.007
10. Chen Z, Chen J, Chen H, Su Z. Evaluation of renal fibrosis in patients with chronic kidney disease by shear wave elastography: a comparative analysis with pathological findings. *Abdom Radiol*. 2022;47(2):738–745. doi:10.1007/s00261-021-03351-x
11. Mayerhoefer ME, Materka A, Langs G, et al. Introduction to radiomics. *J Nucl Med*. 2020;61(4):488–495. doi:10.2967/jnumed.118.222893
12. van Timmeren JE, Cester D, Tanadini-Lang S, Alkadhi H, Baessler B. Radiomics in medical imaging-"how-to" guide and critical reflection. *Insights Imaging*. 2020;11(1):91. doi:10.1186/s13244-020-00887-2
13. Wang LF, Wang Q, Mao F, et al. Risk stratification of gallbladder masses by machine learning-based ultrasound radiomics models: a prospective and multi-institutional study. *Eur Radiol*. 2023;33(12):8899–8911. doi:10.1007/s00330-023-09891-8
14. Luo J, Jin P, Chen J, et al. Clinical features combined with ultrasound-based radiomics nomogram for discrimination between benign and malignant lesions in ultrasound suspected supraclavicular lymphadenectasis. *Front Oncol*. 2023;13:1048205. doi:10.3389/fonc.2023.1048205
15. Guo S, Huang X, Xu C, et al. Multiregional radiomic model for breast cancer diagnosis: value of ultrasound-based peritumoral and parenchymal radiomics. *Quant Imaging Med Surg*. 2023;13(5):3127–3139. doi:10.21037/qims-22-939
16. Chen Z, Ying MTC, Wang Y, et al. Ultrasound-based radiomics analysis in the assessment of renal fibrosis in patients with chronic kidney disease. *Abdom Radiol*. 2023;48(8):2649–2657. doi:10.1007/s00261-023-03965-3
17. Su S, Ye J, Ke H, Zhong H, Lyu G, Xu Z. Multimodal ultrasound imaging: a method to improve the accuracy of sentinel lymph node diagnosis in breast cancer. *Front Oncol*. 2024;14:1366876. doi:10.3389/fonc.2024.1366876
18. Urhuț M-C, Săndulescu LD, Ciocâlteu A, Cazacu SM, Dănoiu S. The clinical value of multimodal ultrasound for the differential diagnosis of hepatocellular carcinoma from other liver tumors in relation to histopathology. *Diagnostics*. 2023;13(20):3288. doi:10.3390/diagnostics13203288
19. Liu X, Xiao W, Qiao J, et al. Prediction of lymph node metastasis in endometrial cancer based on color doppler ultrasound radiomics. *Acad Radiol*. 2024;31(11):4499–4508. doi:10.1016/j.acra.2024.07.056

20. Tang Y, Liu X, Zhou W, Qin X. Interpretable machine learning model based on superb microvascular imaging for non-invasive determination of crescent status of IgAN. *J Inflamm Res*. 2024;17:5943–5955. doi:10.2147/JIR.S476716
21. Dai R, Sun M, Lu M, Deng L. Interpretable machine learning models based on shear-wave elastography radiomics for predicting cardiovascular disease in diabetic kidney disease patients. *J Diabetes Investig*. 2024;15(11):1637–1650. doi:10.1111/jdi.14294
22. Meng F, Wu Q, Zhang W, Hou S. Shear-wave elastography-based radiomics nomogram for the prediction of cardiovascular disease in patients with diabetic kidney disease. *Diabetes Metab Syndr Obes*. 2023;16:2705–2716. doi:10.2147/DMSO.S422364
23. Leong SS, Wong JHD, Md Shah MN, et al. Stiffness and anisotropy effect on shear wave elastography: a phantom and in vivo renal study. *Ultrasound Med Biol*. 2020;46(1):34–45. doi:10.1016/j.ultrasmedbio.2019.08.011
24. Gillies RJ, Kinahan PE, Hricak H. Radiomics: images are more than pictures, they are data. *Radiology*. 2016;278(2):563–577. doi:10.1148/radiol.2015151169
25. Qin X, Liu X, Xiao W, Luo Q, Xia L, Zhang C. Interpretable deep-learning model based on superb microvascular imaging for noninvasive diagnosis of interstitial fibrosis in chronic kidney disease. *Acad Radiol*. 2024. doi:10.1016/j.acra.2024.11.067
26. Zhu Y, Meng Z, Fan X, et al. Deep learning radiomics of dual-modality ultrasound images for hierarchical diagnosis of unexplained cervical lymphadenopathy. *BMC Med*. 2022;20(1):269. doi:10.1186/s12916-022-02469-z
27. Meola M, Ibeas J, Lasalle G, Petrucci I. Basics for performing a high-quality color Doppler sonography of the vascular access. *J Vasc Access*. 2021;22(1_suppl):18–31. doi:10.1177/11297298211018060
28. Bamber J, Cosgrove D, Dietrich CF, et al. EFSUMB guidelines and recommendations on the clinical use of ultrasound elastography. Part 1: basic principles and technology. *Ultraschall Med*. 2013;34(2):169–184. doi:10.1055/s-0033-1335205
29. Correas JM, Anglicheau D, Joly D, Gennisson JL, Tanter M, Helenon O. Ultrasound-based imaging methods of the kidney-recent developments. *Kidney Int*. 2016;90(6):1199–1210. doi:10.1016/j.kint.2016.06.042
30. Liu X, Li N, Xu T, et al. Effect of renal perfusion and structural heterogeneity on shear wave elastography of the kidney: an in vivo and ex vivo study. *BMC Nephrol*. 2017;18(1):265. doi:10.1186/s12882-017-0679-2
31. Leong SS, Jalalonmuhali M, Md Shah MN, et al. Ultrasound shear wave elastography for the evaluation of renal pathological changes in adult patients. *Br J Radiol*. 2023;96(1144):20220288. doi:10.1259/bjr.20220288
32. Lin Y, Chen J, Huang Y, Lin Y, Su Z. A methodological study of 2D shear wave elastography for noninvasive quantitative assessment of renal fibrosis in patients with chronic kidney disease. *Abdom Radiol*. 2023;48(3):987–998. doi:10.1007/s00261-022-03753-5
33. Venkatesh SK, Ehman RL. Magnetic resonance elastography of abdomen. *Abdom Imaging*. 2015;40(4):745–759. doi:10.1007/s00261-014-0315-6
34. Peduzzi P, Concato J, Feinstein AR, Holford TR. Importance of events per independent variable in proportional hazards regression analysis. II. Accuracy and precision of regression estimates. *J Clin Epidemiol*. 1995;48(12):1503–1510. doi:10.1016/0895-4356(95)00048-8